

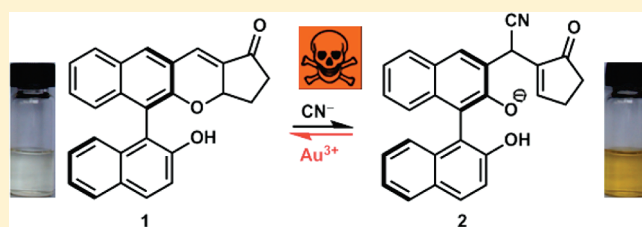
A Selective, Sensitive, and Chromogenic Chemodosimeter for Cyanide Based on the 1,1'-Binaphthyl Scaffold

Yu-Man Dong, Yu Peng,* Ming Dong, and Ya-Wen Wang*

State Key Laboratory of Applied Organic Chemistry, Key Laboratory of Nonferrous Metals Chemistry and Resources Utilization of Gansu Province and College of Chemistry and Chemical Engineering, Lanzhou University, Lanzhou 730000, People's Republic of China

Supporting Information

ABSTRACT: A highly selective chemodosimeter **1** for cyanide based on the 1,1'-binaphthyl skeleton is described which demonstrated significant visual change and a low limit of detection. Interestingly, a reversible process triggered successively by CN^- and Au^{3+} is also observed and determined by fluorescence, UV-vis spectra, ^1H NMR titration, and ESI-MS.



Anions are key to many processes, both industrial and biological, playing crucial roles in both health and the environment.¹ In particular, cyanide salts are widely used in industrial settings such as gold mining, electroplating, and metallurgy (1.5 million tons per year).² However, even very small amounts of the cyanide anion are extremely toxic to living creatures as the result of binding to cytochrome *c* oxidase and inhibition of the mitochondrial electron transport chain;^{3a} any accidental release can result in serious environmental disaster^{3b} especially under potential threats from terrorism. Thus, development of cyanide-selective receptors or fluorescent sensors is in high demand, and previous achievements have been mainly focused on conventional supramolecular approaches⁴ except for some special displacement cases.⁵ Recently, there has been increasing interest in the design of a chemodosimeter for selective recognition to cyanide,⁶ and this usually irreversible reaction-based approach⁷ relies on strong nucleophilicity of CN^- (Figure 1), which has been successfully utilized by cyanohydrin reaction⁸ and related benzil rearrangement⁹ and addition to iminium^{10a-d} or pyrylium.^{10e} Only a few studies involved Michael addition of CN^- to doubly activated acceptors; namely, two electron-withdrawing groups are necessarily attached to $\text{C}=\text{C}$.¹¹ In contrast, known precedent of monoactivated Michael acceptor is rare;¹² thus, its indicative capacity toward cyanide anion is worth investigating.

The 1,1'-binaphthyl scaffold is very useful in molecular recognition¹³ due to its unique rigid conformation and fluorescence properties. In connection with our continuing research of chemosensors based on this efficient fluorophore,¹⁴ herein we report a highly selective and chromogenic chemodosimeter **1** for CN^- with a low limit of detection (13.0 ppb). Unlike usual irreversible chemodosimeters, the interesting reversible phenomenon triggered by Au^{3+} was also observed first that provided a new fashion for the undeveloped fluorescent sensing of gold ions to date.¹⁵ As shown in Scheme 1, **1** was easily prepared from 2,2'-dihydroxy-1,1'-binaphthyl-3-carbaldehyde^{14b} and cyclopent-2-enone

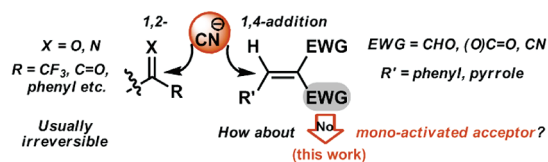
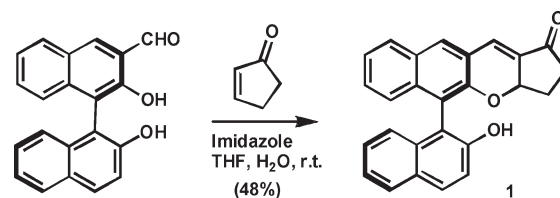


Figure 1. Reaction-based chemodosimeters for cyanide.

Scheme 1. Synthesis of Chemodosimeter 1



via Baylis–Hillman reaction¹⁶ and intramolecular oxa-Michael addition by modifying the reported procedure.¹⁷ Its structure was unambiguously determined by 1D ^1H , ^{13}C NMR, NOE, 2D ^1H – ^1H COSY, IR, and ESI mass spectrometry (Figures S1–S9, Supporting Information).

Next, the Cys, Hys, TGA (thioglycolic acid), *n*-butylamine, F^- , Cl^- , Br^- , I^- , H_2PO_4^- , HSO_4^- , NO_3^- , AcO^- , CF_3SO_3^- , ClO_4^- , BF_4^- , N_3^- , SCN^- , and CN^- were used to measure the selectivity of probe **1** (25 μM) in CH_3CN ,¹⁸ and fluorescence spectra were recorded after 2 min upon addition of 5.0 equiv of each of these anions. Compared to other anions examined, only CN^- generated a fluorescence quench with a slight blue shift from 364 to 356 nm (Figure 2a) when excited at 295 nm. It is surprising that the above thiol species (Cys, Hys, TGA) did not

Received: June 18, 2011

Published: July 13, 2011

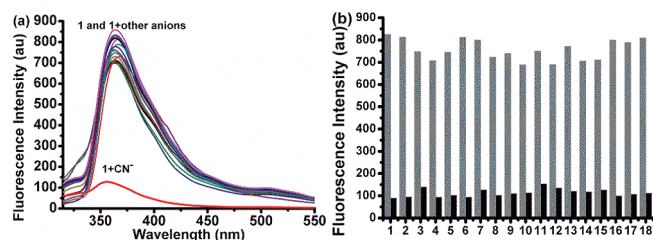


Figure 2. (a) Fluorescence responses of **1** ($25 \mu\text{M}$) with various anions ($125 \mu\text{M}$) in CH_3CN ($\lambda_{\text{ex}} = 295 \text{ nm}$). (b) Selectivity of **1** ($25 \mu\text{M}$). The gray bars represent the emission intensity of **1** in the presence of other anions ($125 \mu\text{M}$). The black bars represent the emission intensity that occurs upon the subsequent addition of $25 \mu\text{M}$ of CN^- to the above solution. From 1 to 15: none, Cys, Hys, TGA, *n*-butylamine, F^- , Cl^- , Br^- , I^- , H_2PO_4^- , HSO_4^- , NO_3^- , AcO^- , CF_3SO_3^- , ClO_4^- , BF_4^- , N_3^- and SCN^- ($\lambda_{\text{em}} = 360 \text{ nm}$).

give interference response since the chromene probes with similar cyclopenta[*b*]-1-one structure exhibited high selectivity for Cys and Hys instead.¹⁹ The best match between the rigid conformation of 1,1'-binaphthyl skeleton and linear (small size) cyanide may be responsible for dramatic switch of selectivity. To validate the selectivity of **1** in practice, the competition experiments were also measured by addition of 1.0 equiv of CN^- to the CH_3CN solutions in the presence of 5.0 equiv of other anions. As shown in Figure 2b, all competitive anions including more nucleophilic competitors such as N_3^- and SCN^- caused no obvious changes, even at the higher concentration ($125 \mu\text{M}$); therefore, the **1**- CN^- system was hardly affected by these coexistent ions. Moreover, a color change from colorless to yellow was observed by the naked-eye upon the addition of cyanide to probe **1**. In the profile of UV-vis spectra, the formation of a new absorption peak at about 375 nm is in good agreement with this color change (Figure S16, Supporting Information). The isosbestic point was not applied as the excitation wavelength since the excitation band and the emission band will overlap to some extent while excited at 334 nm. All of these results suggested that probe **1** displayed an excellent selectivity for CN^- . The corresponding minimum concentration of CN^- for color change²⁰ observed by the naked-eye was further determined to be $2.5 \mu\text{M}$ (65.0 ppb) (Figure S17, Supporting Information). Furthermore, the UV-vis spectra of probe **1** in CH_3CN with different proportions of H_2O were measured and detailed information is attached in Figures S18–S24 (Supporting Information). These results indicated that probe **1** can be used to detect CN^- in aqueous solution even in pure water. Owing to the obvious change of the peak at about 375 nm, behavior of probe **1** in CH_3CN - H_2O (95:5, v/v) was studied in detail. As shown in Figure 3, probe **1** still displayed excellent selectivity for CN^- , and there were no changes at about 375 nm after addition of other ions. This result in CH_3CN - H_2O (95:5, v/v) clearly indicated better selectivity was obtained than that in pure CH_3CN (Figure S16, Supporting Information). The corresponding detection limit in colorimetric mode was determined to be $2.0 \mu\text{M}$ in aqueous solution (Figure S25, Supporting Information).

The fluorescence titrations of CN^- were also conducted using a $25 \mu\text{M}$ solution of **1** in CH_3CN . Upon addition of CN^- to the solution, a significant decrease of the fluorescence intensity at 364 nm was observed (Figure 4a). The total fluorescence intensity of **1** decreased to 15% when 1.0 equiv of CN^- was

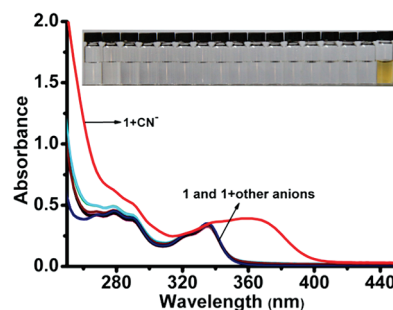


Figure 3. UV-vis spectra of **1** ($25 \mu\text{M}$) with various anions ($125 \mu\text{M}$) in CH_3CN - H_2O (v/v = 95:5). Inset: Color change of **1** ($[\text{I}] = 25 \mu\text{M}$, $[\text{CN}^-] = 50 \mu\text{M}$, [other anions] = $125 \mu\text{M}$). Left to right: **1** only, Cys, Hys, TGA, *n*-butylamine, F^- , H_2PO_4^- , HSO_4^- , AcO^- , NO_3^- , BF_4^- , ClO_4^- , CF_3SO_3^- , N_3^- , SCN^- , and CN^- .

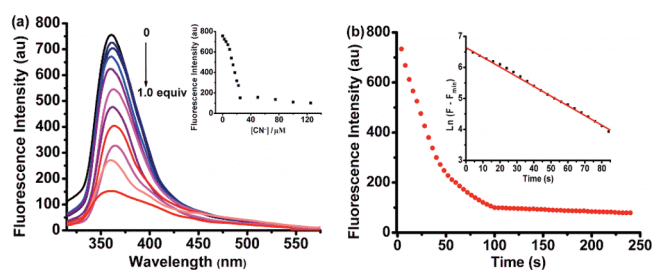


Figure 4. (a) Fluorescence spectra of **1** ($25 \mu\text{M}$ in CH_3CN) upon the addition of CN^- ($\lambda_{\text{ex}} = 295 \text{ nm}$). $[\text{CN}^-] = 0, 2.5, 5.0, 7.5, 10.0, 12.5, 15.0, 17.5, 20.0, 22.5, 25.0 \mu\text{M}$. Inset: Fluorescence intensity at 364 nm as a function of CN^- concentration. (b) The kinetic study of the response of **1** ($25 \mu\text{M}$) to CN^- ($250 \mu\text{M}$) at $25 \text{ }^\circ\text{C}$ under pseudo-first-order condition.

present, and further increase in the concentration of CN^- led to no further fluorescence quench, which clearly demonstrated a 1:1 stoichiometry between CN^- and probe **1** and indicated a chemodosimetric fluorescence change. The 1:1 reaction is also confirmed by ESI-MS (Figure S30, Supporting Information), in which a peak at m/z 422.2 assigned to $[\text{I} + \text{CN} + \text{H}_2\text{O}]^-$ was observed. The corresponding detection limit in fluorescent mode²¹ was determined to be $0.5 \mu\text{M}$ (13.0 ppb) (Figure S26, Supporting Information), which is lower than the WHO guideline of $2.7 \mu\text{M}$ (70.2 ppb) cyanide.²² The kinetic study of the response of CN^- ($250 \mu\text{M}$) to probe **1** ($25 \mu\text{M}$) in CH_3CN at $25 \text{ }^\circ\text{C}$ was measured (Figure 4b). The reaction was finished within 100 s, and the rate constant was obtained by fitting the initial fluorescent intensity changes according to a pseudofirst-order kinetics equation. The observed rate constant at $25 \text{ }^\circ\text{C}$ was estimated to be $k_{\text{obs}} = 0.03 \text{ s}^{-1}$ with $t_{1/2} = 23 \text{ s}$, indicating that probe **1** can react rapidly with CN^- under these experimental conditions.

The response of probe **1** was also investigated by ^1H NMR spectroscopic analysis (Figure 5b,c). With the addition of CN^- (1.2 equiv) to probe **1** in $\text{DMSO}-d_6$ ($25 \text{ }^\circ\text{C}$), the signal of H1 (7.49 ppm) shifted to upfield (5.85 ppm), while the signal of H2 (5.78 ppm) shifted to downfield (7.76 ppm). These results implied the formation of the ring-opened compound **2** (Figures S27–S29, Supporting Information), which may be explained as the 1,4-nucleophilic addition of CN^- to double bond of probe **1**, followed by rapid opening of pyran ring

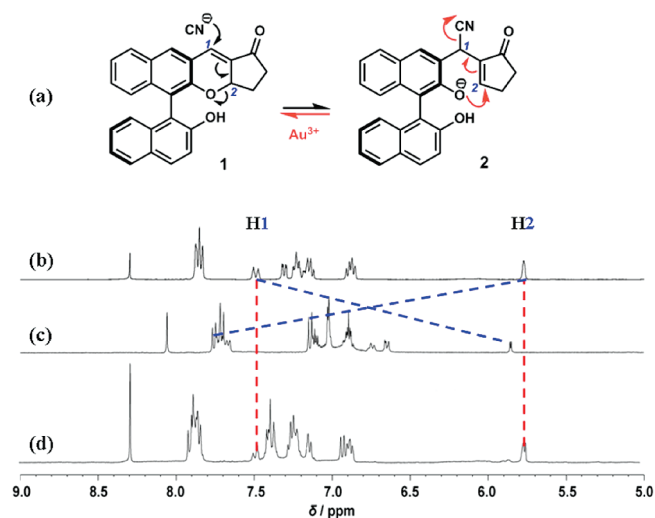


Figure 5. (a) Proposed mechanism. Partial ¹H NMR (400 MHz) spectral change of the probe **1** (20 mM) in DMSO-*d*₆: (b) **1** only; (c) **1** + CN⁻ (1.2 equiv); (d) **1** + CN⁻ + Au³⁺ (0.25 equiv).

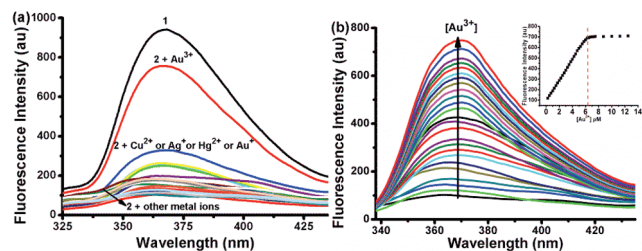


Figure 6. (a) Fluorescence spectral changes of **2** (25 μM) in CH₃CN upon addition of various metal ions (125 μM), including Na⁺, K⁺, Mg²⁺, Ca²⁺, Ba²⁺, Al³⁺, Mn²⁺, Co²⁺, Ni²⁺, Zn²⁺, Cd²⁺, Pb²⁺, Pd²⁺, Cr³⁺, Fe³⁺, Cu²⁺, Ag⁺, Hg²⁺, Au⁺, and Au³⁺. (b) Fluorescence spectral changes of **2** (25 μM) in CH₃CN upon addition of Au³⁺ (λ_{ex} = 295 nm). [Au³⁺] = 0–6.25 μM. Inset: Fluorescence intensity at 364 nm as a function of Au³⁺ concentration.

(Figure 5a, black). Mass spectrometry analysis also supported the existence of **2** (vide supra, see also Figures S30, Supporting Information). This naphthoxide species is responsible for the observed fluorescence change. To verify the hypothesis to identity of **2** further, a large-scale experiment was carried out (see the Experimental Section), and the pure neutral compound **2'** was isolated and characterized by ¹H/¹³C NMR and mass spectrometry (Figures S32–34, Supporting Information). Guided from well-known strong affinity between gold and cyanide, we surmised that the compound **2** may return back to **1** upon the addition of Au³⁺. To our delight, the reversible process did happen and can be rationalized by intramolecular oxa-S_N2' cyclization pathway triggered by Au³⁺ (Figure 5a, red). Except for the analysis of thin-layer chromatography (Figure S31, Supporting Information), this reversible process was also monitored by the ¹H NMR spectrum (Figure 5d). With the addition of Au³⁺ to the DMSO-*d*₆ solution of the **1**–CN⁻ system (**2**), the signals of H1 and H2 were shifted back to 7.49 and 5.78 ppm again, respectively. ESI mass spectrometry analysis (vide infra, see also Figure S36, Supporting Information) confirmed the regeneration of **1** as well.

These results strongly demonstrated that probe **1** not only can detect cyanide but also could be reversible by the addition of Au³⁺. Some features of the whole sensing event are noteworthy: (1) the above reversible process triggered by Au³⁺ is distinctively different from the cases relying on reversible formation of cyanohydrin in the sensing of cyanide where intramolecular H–bond played an important role;²³ (2) this interesting recognition system can be seen as another molecular machine made up of “lock”, “key”, and “hand”;^{19b} (3) recognition of Au³⁺ (vide infra, Figure 6) is dependent on the formation of **2** as a result of recognition of CN⁻, and this combination fashion can be defined as “anion→metal ion approach” contrast to usual demetalation of preassembled complex (“metal ion→anion approach”).^{5,24}

Finally, the responses of **2** to various metal ions were also studied by fluorescence spectra (Figure 6). Upon the addition of these metal ions to the CH₃CN solution of **2**, only Au³⁺ caused the remarkable increase of the fluorescence emission band, which provides an alternative new approach for the undeveloped fluorescent sensing of gold ions.¹⁵ Inevitably, Cu²⁺, Ag⁺, Hg²⁺, and Au⁺ also increased the emission intensity to a small extent, respectively (Figure 6a). The faint response of Cu²⁺ and Ag⁺ could be attributed to a similar affinity to cyanide²⁵ because they belong to the same group (IB) of the modern Periodic Table.²⁶ As the adjacent element to gold in the fifth period, Hg²⁺ also faint response due to common electronic properties in the valence shell.²⁷ Other metal ions such as Na⁺, K⁺, Mg²⁺, Ca²⁺, Ba²⁺, Al³⁺, Mn²⁺, Co²⁺, Ni²⁺, Zn²⁺, Cd²⁺, Pd²⁺, Pb²⁺, Cr³⁺, and Fe³⁺ did not generate the obvious fluorescence enhancement (Figure 6a). Fluorescence titrations of Au³⁺ were carried out (Figure 6b). Upon the addition of Au³⁺ to the solution of **2**, the fluorescence intensity at 364 nm was enhanced. The maximum fluorescence intensity was observed when 0.25 equiv of Au³⁺ was present, and a further increase in the concentration of Au³⁺ led to no further fluorescence enhancement, which demonstrated a 1:4 stoichiometry for Au³⁺ and **2**. This ratio was also supported by ¹H NMR titration experiments and negative-ion ESI mass spectrometry analysis²⁸ (Figures S35 and S36, Supporting Information). The corresponding detection limit was determined to be 0.5 μM (98.5 ppb) (Figure S37, Supporting Information). The corresponding changes of the UV–vis spectra were also shown in Figures S38 and S39 (Supporting Information). With increasing concentration of Au³⁺, the absorption peak at about 375 nm gradually decreased. Furthermore, the changes of UV–vis spectra in CH₃CN–H₂O (95:5, v/v) were also studied in detail (Figure S40 and S41, Supporting Information). The observed rate constant at 25 °C was estimated to be *k*_{obs} = 0.12 min⁻¹ with *t*_{1/2} = 5.7 min (Figure S42, Supporting Information).

In summary, we have developed a highly selective, sensitive, and fluorescent chemodosimeter **1** for CN⁻ with significant visual change. In particular, F⁻ with strong basicity, N₃⁻ and SCN⁻ with strong nucleophilicity, and thiol species did not afford any obvious interference response. Moreover, an interesting reversible process triggered by Au³⁺ with the **1**–CN⁻ system generated after recognition of cyanide is also observed first that provides an alternative choice for the fluorescent sensing of this noble metal ion.

EXPERIMENTAL SECTION

Unless otherwise noted, materials were obtained from commercial suppliers and were used without further purification. Acetonitrile used was purified by distillation. Stock solutions (5 mM) of the tetrabutyl

ammonium salts of F^- , $H_2PO_4^-$, BF_4^- , Cl^- , Br^- , I^- , AcO^- , ClO_4^- , $CF_3SO_3^-$, NO_3^- , HSO_4^- , N_3^- , SCN^- , and CN^- were prepared in CH_3CN . Stock solutions (5 mM) of the perchlorate salts of Na^+ , K^+ , Mg^{2+} , Ca^{2+} , Ba^{2+} , Al^{3+} , Mn^{2+} , Co^{2+} , Ni^{2+} , Zn^{2+} , Cd^{2+} , Pb^{2+} , Cr^{3+} , Fe^{3+} , Cu^{2+} , Ag^+ , Hg^{2+} , and the chloride salts of Au^+ and Pd^{2+} were prepared in ethanol. Stock solutions (5 mM) of Cys, Hys, TGA, *n*-butylamine, and the chloride salt of Au^{3+} were prepared in CH_3CN . A stock solution of **1** (5 mM) was also prepared in CH_3CN . Test solutions were prepared by placing 10 μ L of the probe stock solution into a test tube, adding an appropriate aliquot of each ions stock, and diluting the solution to 2 mL with CH_3CN . For all measurements, the fluorescence spectra were obtained by excitation at 295 nm. Both the excitation and emission slit widths were 5 nm, respectively. Fluorescence spectra were measured after 2 min upon the addition of CN^- and after 20 min upon the addition of Au^{3+} , respectively.

Synthesis of the Probe 1. A yellow solution of 2,2'-dihydroxy-1,1'-binaphthyl-3-carbaldehyde (314 mg, 1 mmol), cyclopent-2-enone (164 mg, 2 mmol), and imidazole (68 mg, 1 mmol) in THF (1.5 mL) at room temperature was mixed with deionized water (0.5 mL). The mixture was stirred at ambient temperature for 3 days and then was diluted by water (10 mL) and extracted with ethyl acetate (3×15 mL). The organic layer was concentrated under reduced pressure. The crude product was purified by flash chromatography (Pet/EtOAc = 4 : 1) on silica gel to give 180 mg of **1** (48% yield). 1H NMR (DMSO- d_6 , 400 MHz): δ 8.31 (s, 1H), 7.86 (t, J = 8.8 Hz, 3H), 7.50 (d, J = 12.0 Hz, 1H), 7.32 (dd, J = 8.8, 2.4 Hz, 1H), 7.25 (t, J = 8.0 Hz, 2H), 7.15 (q, J = 8.0 Hz, 2H), 6.89 (q, J = 8.0 Hz, 2H), 5.78 (brs, 1H), 2.57–2.54 (m, 2H), 2.42–2.38 (m, 2H) ppm; there is no signal of OH and it is determined by exchange experiment with D_2O . ^{13}C NMR (DMSO- d_6 , 100 MHz): δ 207.6, 160.2, 159.8, 153.6, 147.8, 134.3, 134.2, 133.1, 131.5, 131.4, 129.1, 128.3, 128.0, 127.9, 125.9, 125.8, 125.6, 124.3, 122.6, 122.3, 118.7, 116.2, 114.4, 63.7, 34.9, 26.2 ppm. ESI–MS: m/z = 379.2 $[M + H]^+$. IR (KBr): ν_{max} = 3344, 3056, 2921, 1684, 1622, 1595, 1506, 1434, 1384, 1342, 1251, 1198, 1134, 1052, 964, 931, 818, 751 cm^{-1} . HRMS (ESI): calcd for $C_{26}H_{19}O_3^+ [M + H]^+$ 379.1329, found 379.1333.

Characterization of 2. 1H NMR (DMSO- d_6 , 25 $^\circ C$, 400 MHz): δ 8.06 (s, 1H), 7.76 (d, J = 8.0 Hz, 1H), 7.71 (d, J = 8.8 Hz, 2H), 7.67 (d, J = 8.0 Hz, 1H), 7.15–7.09 (m, 1H), 7.03–7.00 (m, 2H), 6.95–6.86 (m, 2H), 6.74 (d, J = 8.0 Hz, 1H), 6.64 (d, J = 8.4 Hz, 1H), 5.85 (d, J = 3.2 Hz, 1H), 2.38–2.32 (m, 2H), 2.27–2.22 (m, 2H) ppm. ^{13}C NMR (DMSO- d_6 , 25 $^\circ C$, 100 MHz): δ 194.2, 170.5, 167.6, 166.2, 157.8, 138.1, 134.4, 134.0, 130.3, 129.5, 128.5, 127.9, 127.73, 127.69, 127.3, 126.7, 126.2, 125.0, 124.6, 123.4, 122.2, 119.6, 119.5, 119.2, 26.2, 24.6, 20.9 ppm. ESI–MS: m/z = 422.2 $[M + H_2O]^+$, calcd for $C_{27}H_{20}NO_4 = 422.2$. HRMS (ESI): calcd for $C_{27}H_{20}NO_4^- [M + H_2O]^-$ 422.1387, found 422.1390.

Synthesis of 2'. Probe **1** (10 mg, 0.026 mmol) and NaCN (1.5 mg, 0.031 mmol) were dissolved in CH_3CN (3 mL) in a flask. The reaction mixture was stirred for 1 h at room temperature and then quenched by water. The mixture was extracted with EtOAc (3×5 mL) and dried over sodium sulfate. The organic layer was concentrated under reduced pressure. The crude product was purified by flash chromatography (Pet/EtOAc = 4:1) on silica gel to give 9.6 mg of **2'** (91% yield). 1H NMR (DMSO- d_6 , 25 $^\circ C$, 400 MHz): δ 10.32 (s, 1H), 8.59 (s, 1H), 8.30 (s, 1H), 8.11–8.09 (m, 1H), 7.90 (d, J = 8.8 Hz, 1H), 7.86 (d, J = 8.0 Hz, 1H), 7.41–7.37 (m, 2H), 7.32 (d, J = 8.8 Hz, 1H), 7.25 (t, J = 8.0 Hz, 1H), 7.18 (t, J = 8.0 Hz, 1H), 7.01–6.97 (m, 1H), 6.92 (d, J = 8.0 Hz, 1H), 5.55 (s, 1H), 2.77–2.68 (m, 1H), 2.67–2.62 (m, 1H), 2.40–2.31 (m, 1H), 2.30–2.21 (m, 1H) ppm. ^{13}C NMR (DMSO- d_6 , 25 $^\circ C$, 100 MHz): δ 196.9, 170.5, 167.6, 166.2, 157.8, 153.3, 137.1, 136.2, 133.8, 130.1, 129.8, 129.3, 128.1, 128.0, 127.2, 126.2, 124.6, 123.9, 123.9, 123.0, 122.5, 118.6, 117.9, 113.5, 26.6, 24.6, 23.1 ppm. EI–MS: m/z = 405 $[M]^+$. IR (KBr): ν_{max} = 3401 (–OH), 3225 (–OH), 3056, 2923, 2852, 2245 (–CN), 1657 (–C=O), 1627 (–C=C), 1599, 1507, 1438, 1340,

1265, 1177, 1137, 1060, 965, 934, 891, 817, 739 cm^{-1} . HRMS (ESI): calcd for $C_{27}H_{20}NO_3^+ [M + H]^+$ 406.1438, found 406.1441.

ASSOCIATED CONTENT

S Supporting Information. UV–vis spectra, the detection limit plots, and copies of $^1H/^{13}C$ NMR, 2D 1H – 1H COSY, and ESI–MS. This material is available free of charge via the Internet at <http://pubs.acs.org>.

AUTHOR INFORMATION

Corresponding Author

*E-mail: pengyu@lzu.edu.cn; ywwang@lzu.edu.cn.

ACKNOWLEDGMENT

This work was supported by NSFC (No. 21001058), the “111” Project of MoE, and the Fundamental Research Funds for the Central Universities (lzujbky-2010-38). We thank Prof. Liming Zhang of UCSB for a generous donation of the textbook to Dr. Yu Peng for his teaching.

REFERENCES

- (1) For a themed issue on “Supramolecular Chemistry of Anionic Species” recently edited by Gale and Gunnaugsson, see: Gale, P. A.; Gunnaugsson, T. *Chem. Soc. Rev.* **2010**, *39*, 3581–4008.
- (2) Young, C.; Tidwell, L.; Anderson, C. *Cyanide: Social Industrial and Economic Aspects*; Minerals, Metals, and Materials Society: Warrendale, 2001.
- (3) (a) Kulig, K. W. *Cyanide Toxicity*; U.S. Department of Health and Human Services: Atlanta, GA, 1991. (b) Koenig, R. *Science* **2000**, *287*, 1737–1738.
- (4) For a tutorial review, see: Xu, Z.; Chen, X.; Kim, H. N.; Yoon, J. *Chem. Soc. Rev.* **2010**, *39*, 127–137 and references cited therein.
- (5) (a) Zeng, Q.; Cai, P.; Li, Z.; Qin, J.; Tang, B. Z. *Chem. Commun.* **2008**, 1094–1096. (b) Chung, S.-Y.; Nam, S.-W.; Lim, J.; Park, S.; Yoon, J. *Chem. Commun.* **2009**, 2866–2868.
- (6) For a tutorial review, see: Cho, D.-G.; Sessler, J. L. *Chem. Soc. Rev.* **2009**, *38*, 1647–1662.
- (7) For a recent review about a reaction-based sensing approach, see: Jun, M. E.; Roy, B.; Ahn, K. H. *Chem. Commun.* **2011**, *47*, 7583–7601.
- (8) (a) Lee, K.-S.; Kim, H.-J.; Kim, G.-H.; Shin, I.; Hong, J.-I. *Org. Lett.* **2008**, *10*, 49–51. (b) Kwon, S. K.; Kou, S.; Kim, H. N.; Chen, X.; Hwang, H.; Nam, S.-W.; Kim, S. H.; Swamy, K. M. K.; Park, S.; Yoon, J. *Tetrahedron Lett.* **2008**, *49*, 4102–4105.
- (9) Cho, D.-G.; Kim, J. H.; Sessler, J. L. *J. Am. Chem. Soc.* **2008**, *130*, 12163–12167.
- (10) (a) Tomasulo, M.; Raymo, F. M. *Org. Lett.* **2005**, *7*, 4633–4636. (b) Yang, Y.-K.; Tae, J. *Org. Lett.* **2006**, *8*, 5721–5723. (c) Shiraishi, Y.; Adachi, K.; Itoh, M.; Hirai, T. *Org. Lett.* **2009**, *11*, 3482–3485. (d) Kim, H.-J.; Ko, K. C.; Lee, J. H.; Lee, J. Y.; Kim, J. S. *Chem. Commun.* **2011**, *47*, 2886–2888. (e) García, F.; García, J. M.; García-Acosta, B.; Martínez-Mañez, R.; Sancenón, F.; Soto, J. *Chem. Commun.* **2005**, 2790–2792.
- (11) (a) Hong, S.-J.; Yoo, J.; Kim, S.-H.; Kim, J. S.; Yoon, J.; Lee, C.-H. *Chem. Commun.* **2009**, 189–191. (b) Kim, G.-J.; Kim, H.-J. *Tetrahedron Lett.* **2010**, *51*, 185–187. (c) Kim, G.-J.; Kim, H.-J. *Tetrahedron Lett.* **2010**, *51*, 2914–2916.
- (12) Recently, Kim et al. reported a special case in which the intramolecular H-bond played an important activation role. For details, see: Park, S.; Kim, H.-J. *Chem. Commun.* **2010**, 9197–9199.
- (13) For a review, see: Pu, L. *Chem. Rev.* **2004**, *104*, 1687–1716.
- (14) (a) Ma, T.-H.; Dong, M.; Dong, Y.-M.; Wang, Y.-W.; Peng, Y. *Chem.—Eur. J.* **2010**, *16*, 10313–10318. (b) Dong, M.; Ma, T.-H.; Zhang, A.-J.; Dong, Y.-M.; Wang, Y.-W.; Peng, Y. *Dyes Pigm.* **2010**,

87, 164–172. (c) Ma, T.-H.; Zhang, A.-J.; Dong, M.; Dong, Y.-M.; Peng, Y.; Wang, Y.-W. *J. Lumin.* **2010**, *130*, 888–892.

(15) For reaction-based fluorescent sensing of Au(I)/Au(III) species that appeared concurrently, see: (a) Egorova, O. A.; Seo, H.; Chatterjee, A.; Ahn, K. H. *Org. Lett.* **2010**, *12*, 401–403. (b) Jou, M. J.; Chen, X.; Swamy, K. M. K.; Kim, H. N.; Kim, H.-J.; Lee, S.-g.; Yoon, J. *Chem. Commun.* **2009**, 7218–7220. (c) Yang, Y.-K.; Lee, S.; Tae, J. *Org. Lett.* **2009**, *11*, 5610–5613. (d) Do, J. H.; Kim, H. N.; Yoon, J.; Kim, J. S.; Kim, H.-J. *Org. Lett.* **2010**, *12*, 932–934. For the first ratiometric case from our group, see: (e) Dong, M.; Wang, Y.-W.; Peng, Y. *Org. Lett.* **2010**, *12*, 5310–5313. For a recent example, see: (f) Yuan, L.; Lin, W.; Yang, Y.; Song, J. *Chem. Commun.* **2011**, *47*, 4703–4705.

(16) For a recent review, see: Wei, Y.; Shi, M. *Acc. Chem. Res.* **2010**, *43*, 1005–1018.

(17) Lee, K. Y.; Kim, J. M.; Kim, J. N. *Bull. Korean Chem. Soc.* **2003**, *24*, 17–18.

(18) The fluorescence behaviors of **1** in other solvents or mixed aqueous solution were so weak that they could not be used to detect CN^- . For details, see Figures S10–S15 (Supporting Information).

(19) It is noteworthy that Yin et al. did not provide the result with the addition of CN^- in their interference experiments; for details, see: (a) Huo, F.-J.; Sun, Y.-Q.; Su, J.; Chao, J.-B.; Zhi, H.-J.; Yin, C.-X. *Org. Lett.* **2009**, *11*, 4918–4821. (b) Huo, F.-J.; Sun, Y.-Q.; Su, J.; Yang, Y.-T.; Yin, C.-X.; Chao, J.-B. *Org. Lett.* **2010**, *12*, 4756–4759.

(20) For the method employed for the detection of limit in colorimetric mode, see: Han, C.; Zhang, L.; Li, H. *Chem. Commun.* **2009**, 3545–3547.

(21) For the method employed for the detection of limit in fluorescent mode, see: Chatterjee, A.; Santra, M.; Won, N.; Kim, S.; Kim, J. K.; Kim, S. B.; Ahn, K. H. *J. Am. Chem. Soc.* **2009**, *131*, 2040–2041.

(22) *Guidelines for Drinking-Water Quality*, 3rd ed.; World Health Organization: Geneva, 2004.

(23) (a) Chung, Y. M.; Raman, B.; Kim, D.-S.; Ahn, K. H. *Chem. Commun.* **2006**, 186–188. (b) Ekmekci, Z.; Yilmaz, M. D.; Akkaya, E. U. *Org. Lett.* **2008**, *10*, 461–464. (c) Kim, D.-S.; Chung, Y. M.; Jun, M.; Ahn, K. H. *J. Org. Chem.* **2009**, *74*, 4849–4854. (d) Jo, J.; Lee, D. *J. Am. Chem. Soc.* **2009**, *131*, 16283–16291.

(24) For a review, see: Nguyen, B. T.; Anslyn, E. V. *Coord. Chem. Rev.* **2006**, *250*, 3118–3127.

(25) (a) For $\text{Cu}(\text{CN})_x^{n-}$ complex formation, see ref 5. (b) For a similar reaction involving decyanation–alkylation triggered by Ag^+ , see: Katoh, T.; Kirihara, M.; Nagata, Y.; Kobayashi, Y.; Arai, K.; Minami, J.; Terashima, S. *Tetrahedron* **1994**, *50*, 6239–6258.

(26) For a special issue on these coinage metals, see: Lipshutz, B. H.; Yamamoto, Y. *Chem. Rev.* **2008**, *108*, 2793–3442.

(27) Gorin, D. J.; Toste, F. D. *Nature* **2007**, *446*, 395–403 and references cited therein.

(28) The mass spectrum of **2** + AuCl_3 displayed two main peaks at m/z 395.3 [**1** + H_2O – H] $^-$ and 301.2 for $[\text{Au}(\text{CN})_4]^-$ except protonation of **2**. See Figures S36 for details. For a similar observation of this auricyanide complex under biomimetic conditions, see: Yangyuoru, P. M.; Webb, J. W.; Shaw, C. F., III. *J. Inorg. Biochem.* **2008**, *102*, 576–583.